AIAA JOURNAL
Vol. 32, No. 4, April 1994

Application of a *p*-Version Finite Element Code to Analysis of Cracks

A. F. Liu* and J. J. Gurbach†
Rockwell International North American Aircraft, Los Angeles, California 90009

A commercially available finite element analysis computer package, i.e., the MECHANICA®-APPLIED STRUCTURE code of the RASNA Corporation, has been used to generate stress intensity solutions for structural damage tolerance analysis applications. A building block approach has been implemented in developing a data reduction technique for using the finite element code. Through two sets of numerical examples, it is demonstrated that stress intensity solutions for the center crack panels (two-dimensional), and the almond shaped cracks (three-dimensional), matched very well with known solutions available in the literature. Stress intensity factors were developed for complex structural geometries for which known stress intensity solutions did not exist. The accuracy of the finite element solutions for cracks (both two- and three dimensional) in a cap-web specimen is demonstrated by correlating the analytically predicted and the experimentally generated crack growth histories.

Introduction

IT has long been recognized that crack tip stress intensity K is the driving force for crack growth and fracture of metallic materials. Damage tolerance analysis (on a real aircraft structure under a specific loading condition) usually treats the local structural area under consideration as if it were the same as a simplified model for which known stress intensity solutions exist. For complex structural configurations where stress intensity solutions are not available, determining K becomes an integral and critical step in performing a structural life predictive analysis.

Among the many analytical techniques being used for determining K, the methods in the finite element category are most suitable to structural analysis application. Using finite elements, the crack is treated as an integral part of the structure, which can then be modeled in as much detail as necessary to accurately reflect the structural load paths both near to and far from the tip of the crack. This technique is particularly useful in modeling the three-dimensional (3-D) (solid type) structures with flaws. Therefore, in recent years, a great deal of attention has been given to the development of finite element methods.

The objective of the present work is to investigate the feasibility of using a commercially available *p*-version finite element package to develop stress intensity factors for structural geometries without any known solution. The following tasks have been performed:

1) The capability (and characteristics) of a selected finite element code, i.e., the APPLIED STRUCTURE section of the MECHANICA® code of the RASNA Corporation, was evaluated through two sets of numerical examples: a) A simple, two-dimensional (2-D) configuration, i.e., a center through crack in a sheet of finite width; and b) a less common, 3-D configuration, i.e., an almond shaped crack at the circumferential notch of a cylinder.

2) Finite element models for a T-beam (of a cap-web configuration) were constructed. Stress intensity factors for cracks of the 2-D and 3-D geometries (depending on the location of the crack) subjected to tension and bending were generated. Crack growth tests of the cap-web specimens (having the same dimensions as the finite element models) were conducted to generate experimental data to assess the accuracy of the finite element stress intensity solutions.

Finite Element Analysis of Cracks

For a stationary crack of a given size, subjected to uniform remote tension load normal to the crack, the displacements along the crack face and the local stresses ahead of the crack tip are, respectively,

$$v = K * \frac{4(1-\mu^2)}{E} * \sqrt{\frac{r}{2\pi}} + \text{higher order terms} \quad (1)$$

for plane strain,

$$v = K * \frac{4\{1-[\mu/(1+\mu)]^2\}}{E} * \sqrt{\frac{r}{2\pi}} + \text{higher order terms} \quad (2)$$

for plane stress, and

$$S_y = K/\sqrt{2\pi r} + \text{higher order terms} \quad (3)$$

regardless of plane strain or plane stress.[1] Here, r is the absolute distance from the crack tip; K the stress intensity; μ the Poisson ratio; and E the elastic tension modulus. The stress intensity K is a function of applied stress, crack size, crack morphology, and structural geometry. Although it is being called the stress intensity factor (by a very loose definition), the stress intensity K, which characterizes the stress and displacement distributions at the crack tip, is a physical quantity (not a factor). Its dimensional unit is in Ksi$\sqrt{\text{inch}}$ (MPa $\sqrt{\text{m}}$). The applied stress is usually defined as the gross area stress (by ignoring the crack, and cutouts, if any) normal to the crack plane unless it is specified otherwise.

The approach to determining K using finite elements is to match the nodal point displacements (or element stresses) with classical crack face displacement, or crack tip stress, solutions [i.e., Eqs. (1), (2), or (3)]. Therefore, it is essential to obtain a stress distribution that accurately simulates the stress singularity at the crack tip. Using a conventional (*h*-version) finite element code, a model containing an extremely

Received Feb. 19, 1993; presented as Paper 93-1450 at the AIAA/ASME/ASCE/AHS/ASC 34th Structures, Structural Dynamics, and Materials Conference, La Jolla, CA, April 19–21, 1993; revision received Aug. 20, 1993; accepted for publication Aug. 23, 1993.

*Senior Engineering Specialist, Durability and Damage Tolerance; mailing address: P.O. Box 4978, West Hills, CA 91308. Associate Fellow AIAA.

†Member of the Technical Staff, Internal Loads.

fine mesh at the vicinity of the crack tip is required. Yet, in many cases, the accuracy has been less than desirable. In the past 20 years, many types of special elements have been developed and published in the literature.[2-8] These special elements were thought to obtain a direct measure of the crack tip stress singularity, or to provide a more accurate account for the stress and displacement fields at the crack tip, or both. It should be noted that more than 90% of this work has dealt with plane elements, i.e., the 2-D geometry. Published work on modeling with solid elements is very limited.

The *p*-version finite element technology, having recently become available, allows stress analysis to be done using coarse mesh, and/or odd shaped elements. By using the *p*-version code, it is conceivable that stress intensity factors can be determined without incorporating any special element at the crack tip. Some characteristics of the *p*-version methodology can be described as follows:

1) In the conventional method, i.e., the *h*-version, the error of approximation is controlled by refining the mesh. In the *p*-version method, the element is described by a group of shape functions of high degree of polynomials (the range can be as high as a nine degree polynomial, as compared to linear or quadratic in the *h*-version), with the flexibility of varying the *p*-level in any designated element.

2) To verify the solution, the *p*-version allows creation of a series of solutions without refining the mesh, as is necessary with the *h*-version. A full sequence of polynomial levels (from one to nine) can be run to allow examination of strain-energy convergence and other functionals of interest. The same mesh is used for all *p*-levels, so no additional effort by the user is required.

3) The user can judge the accuracy of the solution based on converge on stress, or converge on displacement, or both. However, judging from data developed for center crack panels (which will be discussed in the following section), the basis for convergence imposes insignificant impact on stress intensity solutions.

The MECHANICA® code of the RASNA Corporation, which runs on an IBM workstation, was selected to perform all the work for the present investigation. Since it was the only finite element code used, we will just refer to it as PFEM (abbreviated for *p*-version finite element model), or PFEC (for *p*-version finite element code), whichever is appropriate. To establish confidence in using a new tool to solve fracture mechanics problems, the PFEC was first evaluated for its accuracy on routine stress analysis. Consideration was given to structural details such as a flat sheet containing a circular hole (having different hole diameter to sheet width ratios) subjected to uniform far-field tension stresses. Two models were constructed for each configuration (i.e., for each hole diameter to sheet width ratio). One model contained only four elements, i.e., the panel, containing a circular hole at the center, was divided diagonally into four segments (to show that accurate stress solution can be obtained by using a very coarse mesh). The second model contained fine meshes around the hole for obtaining a detailed local stress distribution. Excellent agreement between the PFEC generated stress distributions and the classical Hirsh/Howland solution was obtained.

The applicability of PFEC to crack analysis was then evaluated by comparing the PFEM solutions (which were developed for several 2-D and 3-D crack configurations) with known solutions available in the literature. Following these, the PFEC was used to develop stress intensity factors for cracks in a T-beam without any known solution. The details of this work are presented in the following sections.

Center Crack Configuration

Six models of the center crack configuration were constructed (i.e., in each model a line crack is symmetrically placed in the middle of a rectangular panel). The total width W was 2 in. (50.8 mm). The crack length to panel width ratio $2a/W$ varies; they were: 0.05, 0.25, 0.4, 0.55, 0.7, and 0.9, respectively. The material properties used were: E = 10,300 Ksi (71,000 MPa), and μ = 0.33. Each panel was subjected to 10 Ksi (68.92 MPa) uniform tension stress (i.e., the applied load divided by the product of the full width times the thickness of the panel).

The current releases of the MECHANICA code (Versions 2.0 and 2.1) do not contain any fracture mechanics extraction procedure. Therefore, users must rely on matching the PFEM solutions with Eqs. (1) and (3), or (2) and (3), whichever case is appropriate. Alternatively, one may use the PFEM output (of stresses and displacements) to compute the crack path independent parameter (commonly known as the *J*-integral); K is then obtained through the relationship:

$$J = K^2 * \beta \tag{4}$$

where $\beta = (1 - \nu^2)/E$ for plane strain and $1/E$ for plane stress. Examples demonstrating the procedures on calculating J are available in the literature.[9-11] It can be realized, through a step by step numerical example (for a problem of a crack coming out from a circular hole) given in Ref. 11, that the *J*-integral method requires a substantial effort in reducing the finite element output data. Therefore, this method was abandoned. The K values (for the center crack panels) presented in the following paragraphs were developed by manipulating the PFEM data using Eqs. (2) and (3), and a method that is based on the change of strain-energy during crack extension. The strain-energy release rate concept is described in a section following the discussion of the stress and displacement methods.

Stress or Displacement Based *K*-Solution

For data reduction, the PFEC allows the user to extract 10 pairs of data points (of stress and displacement) along any preselected line connecting any two nodal points of a given element (e.g., along an edge of the element). The data for all six panels are presented in Figs. 1 and 2. The K value for a given panel was determined by using Eqs. (2) and (3), having the higher order terms omitted. The displacement and stress distributions were computed by assigning a K value into these equations. Iterations were made (by reassigning a different K value each time) until the computed v, or S_y, distribution fits the PFEM data. As shown in Figs. 1 and 2, the analytical solution (for v or S_y) only fits the PFEM data over a narrow range of r, which is not too close to, and not too far away from, the crack tip. This is due, in part, to omission of the higher order terms in the analytic equations, and the limitation of the finite element program in producing a proper stress singularity at the crack tip.

Theoretically the K value (for a given crack) can be directly calculated from the PFEM data (v or S_y), with Eqs. (1-3). Within a range of r where the analytical solution matches the

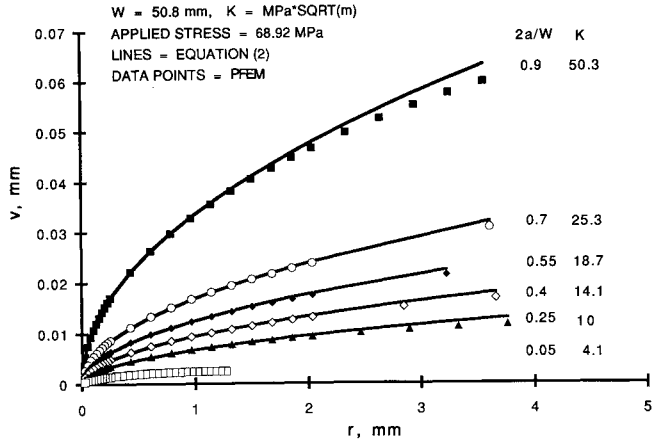

Fig. 1 Crack face displacements for cracks in a center crack panel.

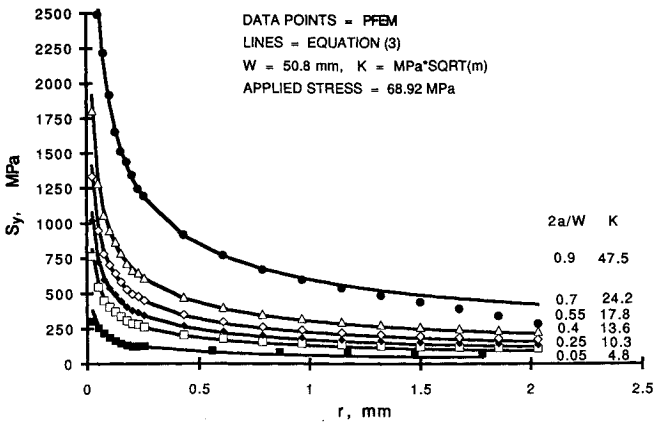

Fig. 2 Crack tip stress distributions for cracks in a center crack panel.

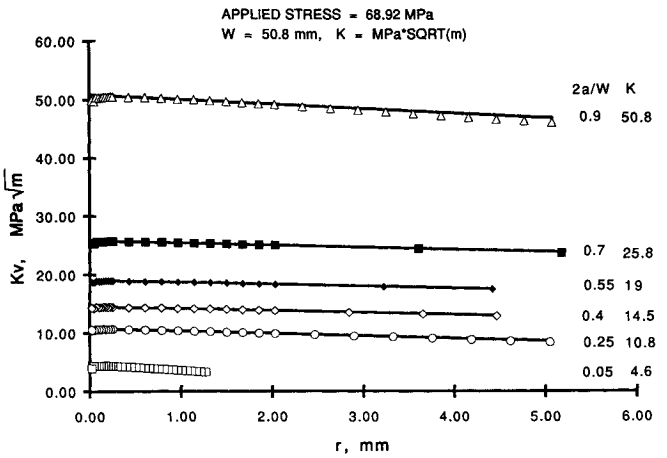

Fig. 3 Center crack stress intensity solutions based on the displacement extrapolation method.

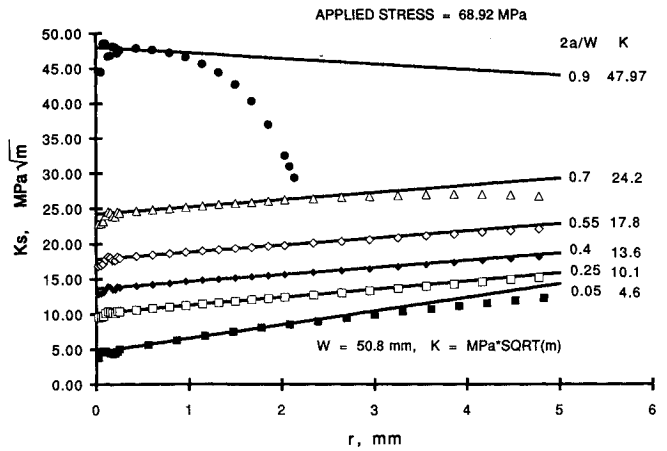

Fig. 4 Center crack stress intensity solutions based on the stress extrapolation method.

finite element solution, K should be a single value. When K is plotted against r, K should be a constant in that region. The plots for this group of center crack panels are shown in Figs. 3 and 4. The Kv and Ks terms (in these figures) implied that the K values are determined based on finite element displacement and finite element stress, respectively. Also shown in these figures are the characteristics of the Kv (or Ks) versus r distribution of which the K values are linear across the region where the analytical and the PFEM solutions correlate. This feature is typical of any finite element analysis results reported in the literature.[7-10] In areas outside the linear region, the computed K values deviate from its regression line and are

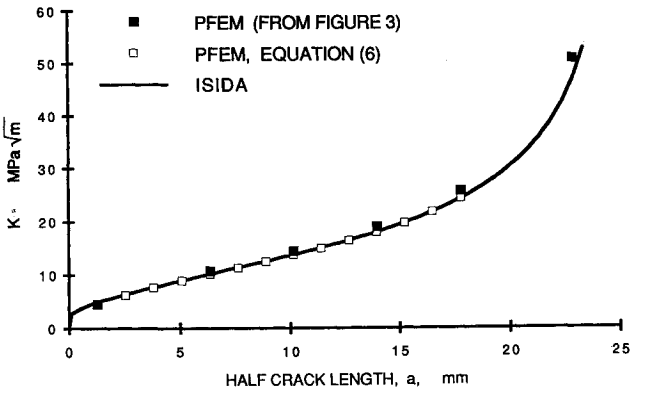

Fig. 5 Comparison of the PFEM and Isida solutions for the center crack panel.

considered to be invalid. The data points inside the linear region can be used as a basis for determining K.

According to Eqs. (1–3), all K values on the regression line should have the same value (i.e., K is a constant). Although not shown in any illustration of this paper, the Kv or Ks values for many crack configurations studied (in this investigation) were indeed a single value. When Kv, or Ks, is not a constant, the real Ks can be obtained by rewriting Eq. (3) as

$$Ks = \sqrt{2\pi r} \lim_{r \to 0} S_y \tag{3a}$$

i.e., by extrapolating the regression line to $r = 0$. The intercept point can be taken as the real K.[9] This same approach can be applied to determine Kv.

Conceptually, all four methods should give an identical K value for a given geometry. In reality, partly due to the computational characteristics of a finite element program, and partly dependent on the configuration under consideration for which the missing higher order terms in the analytical solution might become significantly important, one (or more) of these methods may yield more dependable results than the others.

The K values for all six panels, derived from each of the four data reduction methods, are labeled in Figs. 1–4 along with each fitted curve. In the light of the appearance of these figures, and the figures to be presented later (for the solid element models), it appears that the displacement extrapolation method (i.e., shown in Fig. 3) is consistently better than the others. Therefore, this method has been selected to determine K for all of the crack configurations considered in this paper.

There are many stress intensity solutions for the center crack configuration. Among them, the Isida solution[12] is regarded as being the most accurate by the fracture mechanics community. For comparison purposes the Isida solution is plotted in Fig. 5, together with the finite element solution (which is based on the intercept point of the Kv vs r curve). It is seen that the agreement between the two solutions is excellent.

Strain-Energy Based *K*-Solution

Since the MECHANICA code also computes the strain-energy term for each crack model, therefore, K values can be computed directly from PFEM data, using the known relationship between strain-energy release rate and K, which is

$$G = K^2 * \beta \tag{5}$$

with G being the change in strain-energy per change in crack area. Hence, for a crack of length $(a_1 + a_2)/2$

$$K = \sqrt{(U_2 - U_1)/[(a_2 - a_1) * t * \beta]} \tag{6}$$

where t is the plate thickness, a_1 and a_2 are two successive crack lengths, and U_1 and U_2 are the respective strain-energy values. Thus, this method requires two finite element solutions to generate one value of K. The results for the center cracks are plotted in Fig. 5. Excellent correlation with the Isida solution is also obtained.

Almond Shaped Crack Configuration

To evaluate PFECs capability in developing K with solid elements, an almond shaped crack in a cylindrical cross section was considered. The crack was placed at the root of a circumferential notch, which is located at the midlength of the cylinder. The dimensions that define the crack geometry are: 1) the crack depth, a, and 2) the visible crack length, b (circumferential, see Fig. 6a). Based on experimental data,[13,14] the crack front shape for this type of crack would be an arc of a circle. The center of the circle floats in between the free surface of the cylinder and a point infinitively far away from the cylindrical surface. For crack sizes larger than one half of the minor diameter of the cylinder, d, the crack front eventually became a straight line although a circular shape (by geometric definition) had been maintained at all times.

For a crack having a curved crack front, K values vary along the crack periphery. This variation causes the crack front to grow a different amount in different directions. Consequently, crack shape continuously changes as the crack extends. A two-dimensional (or even a multidimensional) crack growth scheme may be required in making crack growth life predictions. However, it can be simplified by treating the 3-D crack as if it were a 2-D crack. An underlying prerequisite for making such an approximation is the knowledge of crack growth behavior of the crack under consideration, as to the crack geometry (i.e., crack shape aspect ratio) corresponding to every incremental step of crack growth. On the basis of experimental calibrations, on notched cylinders made of 4340 steel, there was a unique relationship between a/b and a/d.[14] Therefore, it is possible to simulate a scenario for multidirectional crack growth if the finite element models are built-in with these predetermined a/b ratios. A reasonably accurate prediction of crack growth life can be obtained by monitoring only one point on the crack periphery (e.g., at the maximum depth). An in-depth discussion of this subject was given in Ref. 15.

Seven models of the almond shaped crack geometry have been constructed. The dimensions of these crack models were: d = 0.886 in. (22.5 mm), a/d = 0.02, 0.0375, 0.22, 0.365, 0.5, and 0.72 (two models), respectively. The a/b ratio for each crack model, except one, was set to exactly the same as those reported in Ref. 14. That is, $a/b \approx 0.65$ for crack sizes up to a/d = 0.5, and a/b = 0.75 for a/d = 0.72. The last model, also for a/d = 0.72, the a/b ratio was set to 0.89 for showing the effect of a/b ratio on K.

Each crack model was subjected to uniaxial tension stress of 12.74 Ksi (87.80 MPa), based on the applied load divided by the minor cross-sectional area of the notched cylinder. The material properties for these models were: E = 29,000 Ksi (0.2E6 MPa), and μ = 0.33. The stress intensity at the maximum depth of the crack was determined using the same data reduction methods described in the previous section. One set of the reduced data (for a/d = 0.365) is shown in Figs. 7 and 8. Again, based on all the data reviewed, the displacement extrapolation method provided the most reliable results.

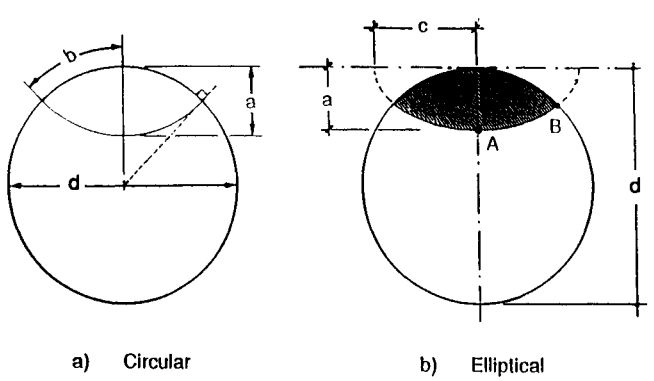

Fig. 6 Nomenclature for an almond shaped crack.

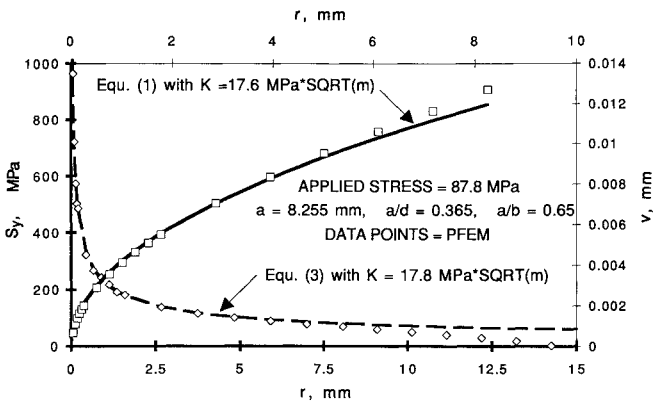

Fig. 7 Crack tip stresses and crack face displacements for an almond shaped crack.

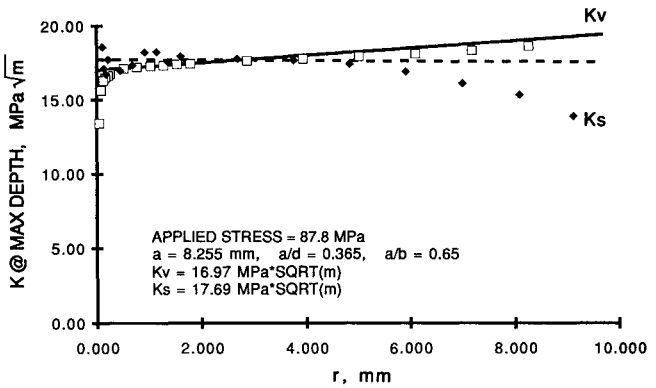

Fig. 8 Stress intensities for an almond shaped crack based on extrapolation methods.

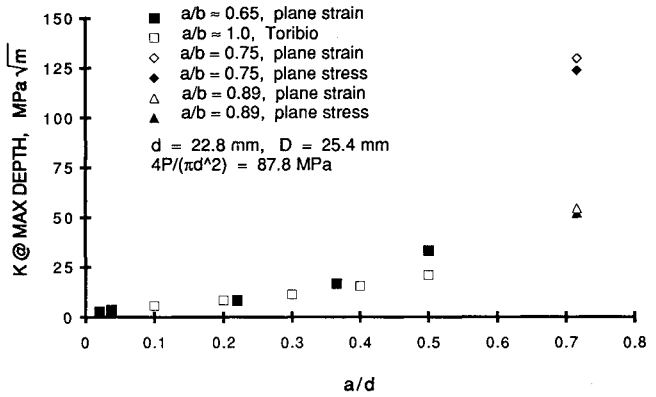

Fig. 9 Comparison of the PFEM and Toribio solutions for the notched cylinder.

The K values for all seven crack models (based on the intercepted Kv method) are presented in Fig. 9. For the first five models, i.e., $a/d \leq 0.5$, the crack front constraint was very high so that a plane strain condition was assumed. That is, Eq. (1) was used to compute v. As the crack gets larger, the crack tip constraint will gradually change from plane strain to plane stress. Therefore, each of the last two models (a/d = 0.72) is presented with two K values, i.e., for both plane stress and plane strain.

Also shown in Fig. 9 are finite element solutions of Toribio et al.[16] It should be noted that the notch root radius in the

finite element models of Ref. 16 was 0.125 mm, whereas the finite element models of the present study had a sharp notch (i.e., the notch root radius was zero). In addition, the crack models of Ref. 16 were of the semicircular crack configuration, centered on the free surface of the cylinder (see Fig. 6b). That is, based on the notation of Fig. 6b, these cracks had a constant a/c ratio of 1.0. This can be translated to a/b ratios between 1.0 and 0.95 for $0 \leq a/d \leq 0.5$. In fact, the 0.89 a/b ratio for the last crack model of this study (for $a/d = 0.72$) was actually translated from $a/c = 1$. It was done this way to have a crack geometry entirely compatible to Toribio's crack models.

For a given a/d ratio the crack that has a lower a/b ratio would have an area larger than a crack of a higher a/b ratio. Therefore, the K value for the former would have been higher than the latter. As a/d increases, the difference in cracked area between the two cracks (of the same a/d ratio, but different a/b ratios) increases, thus the difference in K also increases. This trend is evident in the finite element data shown in Fig. 9. In any event, it can be concluded that within an a/d range where the effect of a/b (on K) is insignificant, the results of the present investigation matched very well with Toribio's three-dimensional finite element solution.

Cap-Web Configuration

Consider a T-beam, i.e., a beam having a T cross section that consists of a huge mass on top, connecting to a thin section at the bottom (see Figs. 10 and 11). This configuration simulates an aircraft longeron, and is referred to as a cap-web configuration. For a crack initiated at the bottom edge of the thin web propagating toward the thick cap, it is conceivable that crack growth rates will be reduced while the crack is adjacent to (or inside) the cap. For a quantitative determination of this phenomenon, an experimental fatigue crack growth test was conducted. A cap-web specimen configuration (shown in Fig. 10) was designed, and cyclically loaded

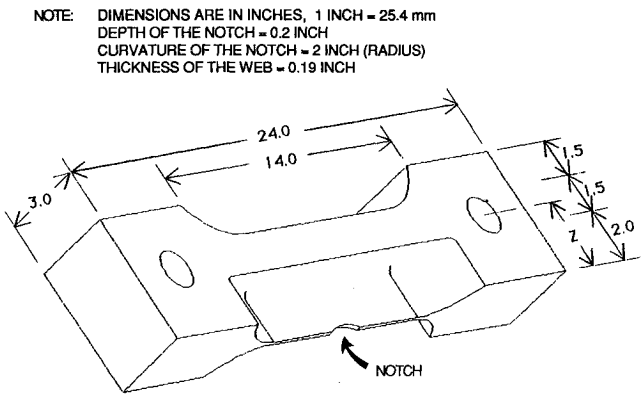

Fig. 10 Three-dimensional view of the cap-web specimen.

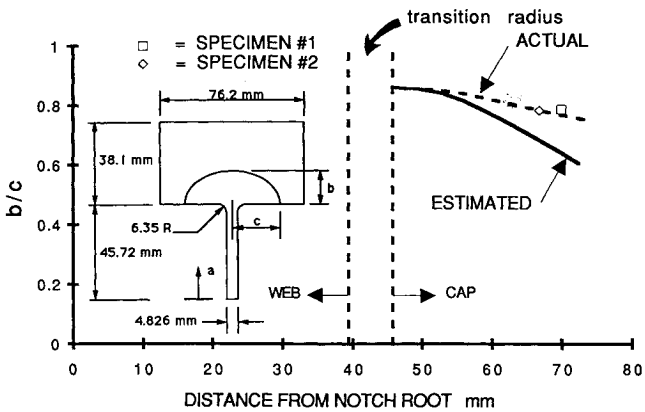

Fig. 11 Comparison of experimental and estimated crack front shape aspect ratios.

in a five hundred thousand pound load (2.225 MN) MTS machine. Axial loads were applied through the pin holes at both ends of the specimen. By altering the position of the pin hole, in respect to the depth direction of the web, i.e., the Z dimension shown in Fig. 10, a variety of combinations in tension and bending were obtained.

The test consisted of constant amplitude cyclic crack growth testing of two cap-web specimens, one subjected to pure tension, another one subjected to combined tension and bending. Prior to experimental testing, analytical determination of specimen cross-sectional stress distributions and stress intensity factors (corresponding to each stress distribution under consideration) for various crack sizes were required. The details of the analytical results, experimental test procedures, and analytical/experimental correlations are described in the following sections.

Loading Conditions

A quarter solid element model having the same overall dimensions as that shown in Fig. 10 has been constructed. By adjusting the center of the pin hole, uncracked stress distributions corresponding to pure tension, and the combination of 74% tension and 26% bending can be obtained. Based on the PFEM results, the Z dimensions corresponding to these loading conditions are 2.631 in. (66.83 mm), and 2.516 in. (63.91 mm), respectively. Cross-sectional stress distributions for these loading cases are presented in Figs. 12 and 13. In obtaining these uncracked stress distributions, uniformly distributed loads were applied to one half of the pin hole simulating the pin to hole contact pressure.

Also shown in Figs. 12 and 13 are strain gauge data obtained from the experimental test program. The details for the strain survey procedures will be discussed in the section for exper-

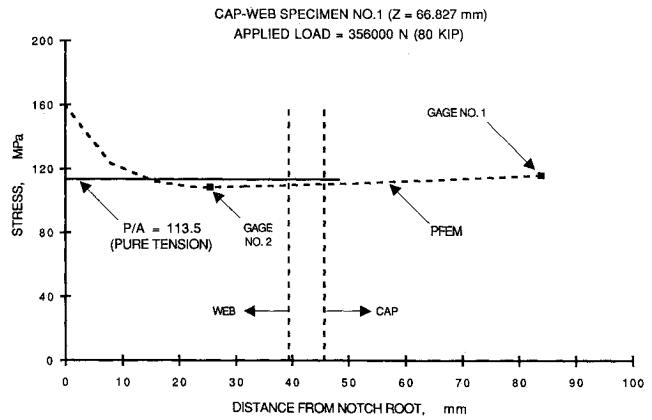

Fig. 12 Stress distribution in cap-web Specimen No. 1.

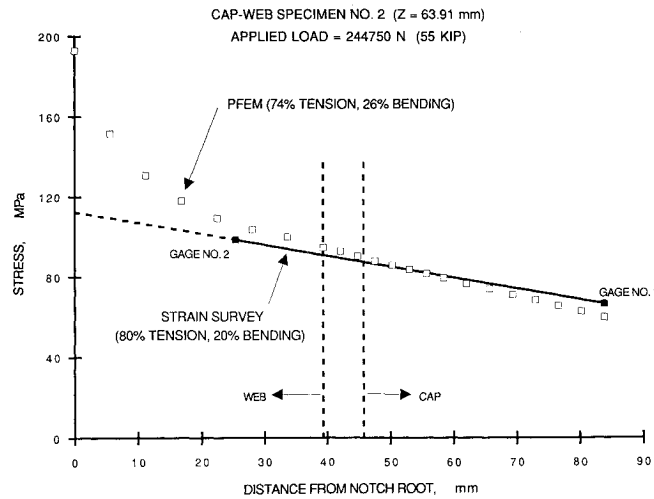

Fig. 13 Stress distribution in cap-web Specimen No. 2.

imental testing. In any event, it is evident that the strain survey data for Specimen No. 1 (i.e., pure tension) perfectly matches the local stress distribution of the PFEM. Close agreement between strain survey and PFEM data was also obtained for the second specimen (i.e., Specimen No. 2). However, by extrapolating the strain gauge data to the notch root, an extreme fiber My/I stress of 16.32 Ksi (112.5 MPa) was obtained. A combination of this stress level and the stress level of 9.71 Ksi (66.9 MPa) on top of the cap (i.e., the data point for strain gauge No. 1) suggested that the actual loading condition on the specimen was 80% tension and 20% bending.

PFEM Stress Intensity Solutions

In the finite element models, cracks were placed at the midlength of the cap-web specimen, starting from the maximum depth of the circular notch and extended into the cap. While the crack is in the web of the cap-web specimen, the crack can be modeled as a through the thickness crack (i.e., having a straight crack front). As the crack penetrates into the cap, the crack will have a shape of a mushroom (i.e., having an elliptical crack front and a stem, see Fig. 11). Thus, a two-dimensional crack growth scheme should be considered. To simplify the crack growth analysis procedure to an equivalently one-dimensional scheme, the idea previously used on the almond shaped crack is also applicable here. Therefore, estimating the crack front shape aspect ratios is a necessary step prior to finite element modeling. This step can be done analytically, by assuming that the crack will stabilize itself (during crack propagation) by continuously adjusting its shape to maintain a nearly uniform K along the elliptical boundary. For a given crack dimension, the amount of K variation (along the crack periphery) depends on the aspect ratio of the ellipse, among other geometric variables on the crack plane. Therefore, the shape aspect ratio that exhibits a uniform K (along the crack boundary) is not a constant for all crack sizes. The crack geometries that can be expected in the cap-web specimen have been estimated using the elliptical flaw solutions of Ref. 17. The results are presented in Fig. 11. These crack shape aspect ratios were used to make finite element models for the mushroom cracks. Stress intensity at the maximum depth (of each crack model) was obtained by reducing the PFEM data in the same manner as discussed earlier.

For cracks subjected to pure tension, an eighty thousand pound load (356,000 N) was applied to the pin hole. Actually, two finite element models had been built for this case, i.e., with and without the notch. For a given applied load, the magnitude of stress varies depending on loading condition. Direct comparison of stress intensities (in between different combinations of tension and bending) cannot be made unless the Ks are normalized by a common denominator, i.e., a reference stress level, S_{ref}. In this case S_{ref} is the nominal P/A stress of 16.47 Ksi (113.5 MPa) given in Fig. 12. As shown in Fig. 14, the PFEM solutions are plotted as K/S_{ref} vs a (instead of K vs a). It shows that the K values are higher in the vicinity of the notch, as compared with a crack of the same length without a notch. The effect of the notch diminishes as the crack becomes longer. As expected intuitively, the magnitude of K decreases when the crack approaches the cap, and eventually increases again as the crack is progressing toward the top of the cap.

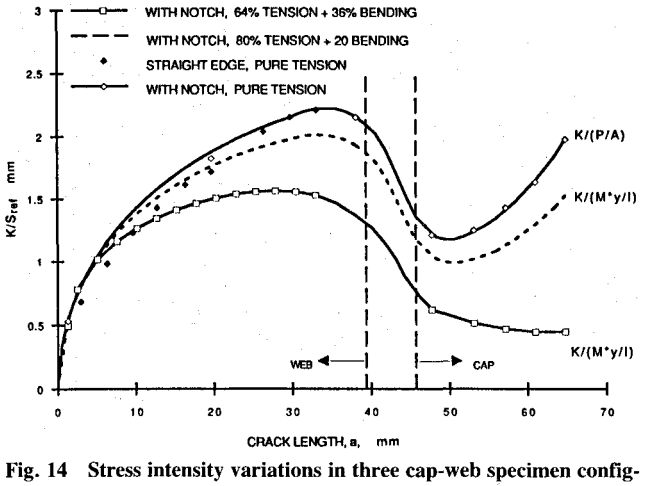

Fig. 14 Stress intensity variations in three cap-web specimen configurations.

To provide flexibility in generating stress intensity solutions for a variety of combined tension and bending without the need for making a PFEM run for each loading condition, stress intensity factors for cracks subjected to bending moment alone were generated. To do this, the loading arm was removed from the finite element model so that bending moment could be applied at the fixed end of the model.

For a bending moment of 20,000 in.-lb (2260 N-m), a hand calculated My/I stress of 26.786 Ksi (184.61 MPa) was obtained at the notch root location (without accounting for stress concentration due to the notch). The bending stress reduced linearly to -9.595 Ksi (-66.13 MPa) on top of the cap. This stress distribution is equivalent to a combination of 64% tension and 36% bending. Using the unnotched extreme fiber stress (i.e., 184.61 MPa) as the reference stress level, the normalized K/S_{ref} values are also plotted (as a function of crack sizes) in Fig. 14.

Based on uncracked stress distribution and strain survey data shown in Fig. 13, loading condition for Specimen No. 2 is considered to be 80% tension plus 20% bending. Stress intensity factors were determined (based on superposition principle), from the stress intensities for tension, and fixed end bending. Using 112.5 MPa (extrapolated from strain survey data, see Fig. 13) as the reference stress level, the K/S_{ref} values for this case are plotted in Fig. 14 along with PFEM data for the other two loading conditions.

Experimental Crack Growth Tests

Constant amplitude fatigue crack growth tests were completed on two cap-web specimens made of the 7075-T7351 aluminum. Both specimens contained a round notch at the midlength of the specimen. One specimen was tested under pure tension, whereas the second specimen was subjected to combined tension and bending. These tests were carefully planned so that the test specimens and the corresponding finite element models would have exactly the same dimensions and be subjected to the same loading conditions.

Test Procedures

1) Specimen No. 1—Pure Tension

This specimen was instrumented with two strain gauges. Both gauges were located at the midlength of the cap-web specimen. One of them was placed on the web (25.4 mm above the maximum depth of the notch). Another strain gauge was placed on top of the cap. Strain survey was conducted at load levels up to 356,000 N, at 4450 N increments, for both uploading and downloading paths.

A crack starter, approximately 1 mm in length, was made by using a jeweler's saw on the bottom edge of the web (at the maximum depth of the notch). It was sharpened to approximately 2 mm by applying constant amplitude load cycles in the same manner as the actual test. That is, the load profile for this test was 356,000 N maximum, with $R = 0.1$ (i.e., 35,600 N, minimum). Cyclic loads were applied at a constant frequency of 10 Hz. Whenever possible, crack length vs number of cycles data were taken at approximately every 4 mm interval. For cracks inside the cap, the visible crack lengths were measured along the bottom of the cap. Test was terminated when the visible crack length exceeded approximately two-thirds of the cap width.

2) Specimen No. 2—Simulated Bending

The center of the loading hole for this specimen was located at $Z = 2.516$ inch (63.91 mm). Although this specimen was

also subjected to an axially applied load, the position of the pin caused the specimen to experience a combined tension and bending. As mentioned earlier, the loading condition for this specimen is considered to be 80% tension plus 20% bending. Test procedure for this test was the same as those specified for Specimen No. 1 except a) the maximum load level for strain survey was limited to 267,000 N and b) the maximum cyclic load level for constant amplitude crack growth was 244,750 N.

Test Results and Correlation with Analytic Predictions

Following the completion of each test, the actual flaw shape aspect ratio for the mushroom shaped crack inside the cap was revealed by examining the crack surfaces of the broken halves of the cap-web specimen. Comparison of the actual and the estimated b/c ratios (as a function of crack length) is given in Fig. 11. Using the actual b/c vs a relationship, the crack lengths measured along the bottom of the cap were translated to crack depths inside the cap. Thus, experimental crack growth history for each test was reduced to a total crack length vs number of cycles format. The final results (i.e., the a vs N curves for both specimens) are presented in Figs. 15 and 16.

Analytically predicted crack growth histories were also generated. They were based on the K-values determined by using the PFEM. Material crack growth rate properties for the 7075-T7351 aluminum were taken from Rockwell's material properties data bank. For $R = 0.1$, it can be defined by a linear

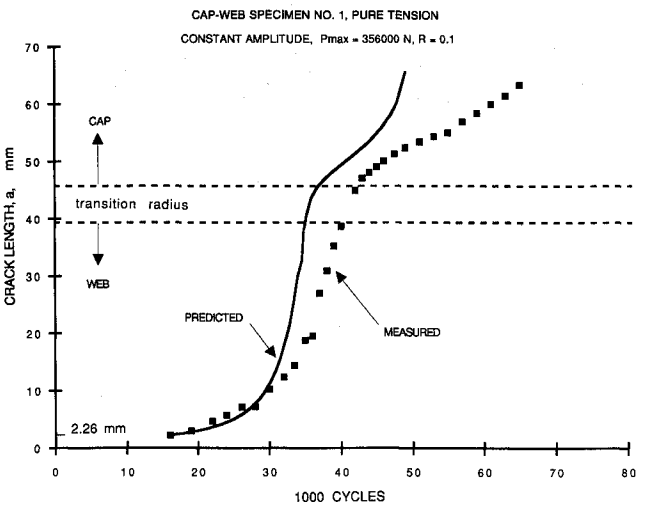

Fig. 15 Comparison of experimental and predicted crack growth histories for cap-web Specimen No. 1.

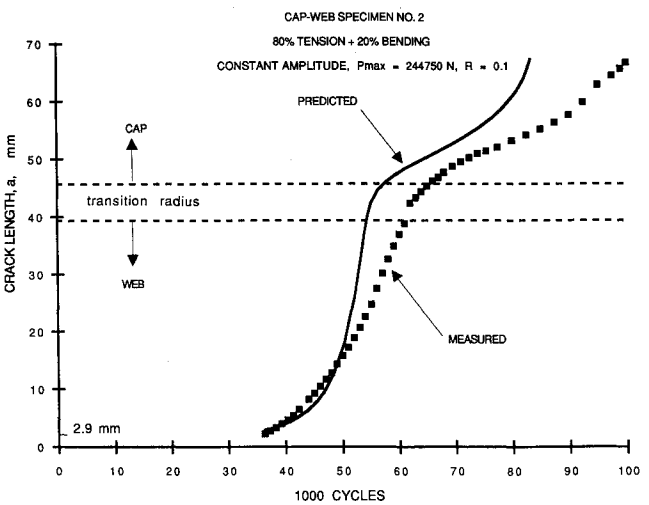

Fig. 16 Comparison of experimental and predicted crack growth histories for cap-web Specimen No. 2.

relationship (on a log-log scale) in between two pairs of da/dN vs ΔK data points as follows:

ΔK (MPa$\sqrt{m}$)	da/dN (m/cycle)
7.36	2.99E-8
49.45	2.90E-5

Comparisons between the analytical predictions and experimental data are shown in Figs. 15 and 16. It appears that the correlations are good. The somewhat conservative appearance in the predicted crack growth histories was attributed to the minor difference between the estimated and the actual crack shape aspect ratios, and lack of PFEM data points (for K) in the transition radius region of the cap-web specimen. Perhaps the major effect actually came from material property scatter because the crack growth rate data used for making the predictions did not come from the same batch of material from which the specimens were made.

Conclusions

The feasibility of using a p-version finite element stress analysis code to develop stress intensity solutions for structural damage tolerance analysis has been investigated. Center crack (2-D) and almond shaped crack (3-D) models were developed by using plane elements and solid elements, respectively. Stress intensity factors reduced from crack face displacement solutions matched very well with known solutions available in the literature.

For complex structural components for which known stress intensity solutions do not exist—for example, cracks in a cap-web specimen—the accuracy of the PFEM solutions was assessed by comparing the analytically predicted and the experimentally developed crack growth histories. Satisfactory correlations were obtained.

References

[1]Irwin, G. R., "Analysis of Stresses and Strains Near the End of a Crack Transversing a Plate," *Journal of Applied Mechanics*, Vol. 24, *Transactions of the American Society of Mechanical Engineers*, Series E, 1957, pp. 361–364.

[2]Tracey, D. M., "Finite Elements for Determination of Crack Tip Elastic Stress Intensity Factors," *Engineering Fracture Mechanics*, Vol. 3, 1971, pp. 255–265.

[3]Tong, P., Pian, T. H. H., and Lasry, S., "A Hybrid-Element Approach to Crack Problems in Plane Elasticity," *International Journal of Numerical Methods in Engineering*, Vol. 7, 1973, pp. 297–308.

[4]Ingraffea, A. R., and Manu, C., "Stress Intensity Factor Computation in Three Dimensions with Quarter-Point Elements," *International Journal for Numerical Methods in Engineering*, Vol. 15, 1980, pp. 1427–1445.

[5]Shih, C. F., deLorenzi, H. G., and German, M. D., "Crack Extension Modeling with Singular Quadratic Isoparametric Elements," *International Journal of Fracture*, Vol. 12, 1976, pp. 647–651.

[6]Raju, I. S., and Newman, J. C., Jr., "Three-Dimensional Finite-Element Analysis of Finite-Thickness Fracture Specimens," NASA TN D-8414, Langley Research Center, Hampton, VA, May 1977.

[7]Banks-sills, L., and Einav, O., "On Singular, Nine-Noded, Distorted, Isoparametric Elements in Linear Elastic Fracture Mechanics," *Computers & Structures*, Vol. 25, No. 3, 1987, pp. 445–449.

[8]Henshell, R. D., and Shaw, K. G., "Crack Tip Finite Elements are Unnecessary," *International Journal for Numerical Methods in Engineering*, Vol. 9, 1975, pp. 495–507.

[9]Chan, S. K., Tuba, I. S., and Wilson, W. K., "On the Finite Element Method in Linear Fracture Mechanics," *Engineering Fracture Mechanics*, Vol. 2, 1970, pp. 1–17.

[10]Banks-sills, L., and Sherman, D., "Comparison of Methods for Calculating Stress Intensity Factors with Quarter Point Elements," *International Journal of Fracture*, Vol. 32, 1986, pp. 127–140.

[11]Shows, D., Liu, A. F., and FitzGerald, J. H., "Application of Resistance Curves to Cracks at a Hole," *Fracture Mechanics: Fourteenth Symposium—Volume II: Testing and Applications*, ASTM STP 791, American Society of Testing and Materials, Philadelphia, PA, 1983, pp. II-87–II-100.

[12]Isida, M., "Stress Intensity Factor of the Tension of an Eccentrically Cracked Strip," *Journal of Applied Mechanics*, Vol. 33, *Transactions of the American Society of Mechanical Engineers*, Series E, 1966, pp. 674–675.

[13]Forman, R. G., and Mettu, S. R., "Behavior of Surface and Corner Cracks Subjected to Tensile and Bending Loads in Ti-6Al-4V Alloy," *Fracture Mechanics: Twenty Second Symposium (Volume I)*, ASTM STP 1131, American Society of Testing and Materials, Philadelphia, PA, 1992, pp. 519–546.

[14]Cervay, R. R., "Empirical Fatigue Crack Growth Data for a Tension Loaded Threaded Fastener," Air Force Wright Aeronautical Labs., AFWAL-TR-88-4002, Feb. 1988.

[15]Liu, A. F., "Behavior of Fatigue Cracks in a Tension Bolt," Symposium on Structural Integrity of Fasteners, American Society for Testing and Materials, Miami, FL, Nov. 18, 1992; also ASTM STP 1236 (to be published).

[16]Toribio, J., Sanchez-Galvez, V., and Astiz, M. A., "Stress Intensification in Cracked Shank of Tightened Bolt," *Theoretical and Applied Fracture Mechanics*, Vol. 15, 1991, pp. 85–97.

[17]Newman, J. C., Jr., and Raju, I. S., "An Empirical Stress-Intensity Factor Equation for the Surface Crack," *Engineering Fracture Mechanics*, Vol. 15, 1981, pp. 185–192.